JOURNAL OF MATERIALS SCIENCE 25 (1990) 4266–4272

Influence of oxygen contamination on the surface tension of liquid tin

A. PASSERONE, E. RICCI, R. SANGIORGI
Istituto di Chimica Fisica Applicata dei Materiali, CNR, Lungobisagno Istria 34, 16141 Genova, Italy

The surface tension of liquid tin has been measured by the sessile-drop technique as a function of temperature, in the range $232 \leqslant T\ (^\circ C) \leqslant 800$ and under different atmospheres. It is shown that oxygen strongly affects the surface tension values and that, under "nominally" very clean conditions, a considerable scatter of experimental results occurs. This scatter can be explained by taking into account kinetic factors, especially those related to the gaseous fluxes around the molten drop. By this procedure, a number of experimental results can be singled out, which corresponds to "clean" surface conditions. On the basis of these results, the following expression for surface tension politherm is proposed:

$$\sigma(\mathrm{mN\,m^{-1}} = 581 - 0.13\ )\ (t - 232).$$

1. Introduction

The surface tension of pure liquid metals is strongly affected by the presence of other elements that segregate to the liquid surfaces. Among such elements, one of the most important is oxygen, due to its nearly "unavoidable" presence in the gaseous environments of technical processes involving liquid metals. For this reason, the influence of oxygen on the surface tension of liquid metals has been rather extensively investigated.

Metals such as iron (see review by Keene [1]), nickel [2], cobalt [3], silver [4–6], copper [7–10], lead [11, 12], silicon [13], gallium [14] and aluminium [15] have been examined, usually at constant temperature, under oxygen partial pressures ranging from very low values up to the saturation of the bulk liquid phase.

As a general rule, when plotting the variation of σ as a function of $\ln X$, where X is the bulk oxygen molar fraction, an S-shaped curve is obtained (Fig. 1), with an initial slow decrease in σ, an intermediate steep dependence of σ on $\ln X$, and a final trend towards a "foot" with a very small slope. The presence of this "foot" is noticeable in certain systems tested under a wide range of oxygen partial pressures. This trend has been demonstrated theoretically [16]. This particularly occurs for silver and copper, which allow experiments to be performed up to fairly high oxygen partial pressures, without saturating the bulk liquid phase. When oxygen solubility decreases, the surface tension varies over a range of oxygen partial pressures which is more and more difficult to explore experimentally.

It has recently been shown [16], that a relationship exists between the oxygen molar fraction at bulk saturation, X_{sat}, and the bulk oxygen content, $X_{\Gamma_{mx}}$, corresponding to the maximum Gibbsian adsorption, $\Gamma_{1,2max}$:

$$\ln \frac{X_{sat}}{X_{\Gamma mx}} \approx 3 \qquad (1)$$

When metals such as aluminium and tin are considered, whose X_{sat} values are very low ($X_{sat} = 8 \times 10^{-10}$ at 700° C for aluminium and $X_{sat} = 1.8 \times 10^{-8}$ at 300° C for tin [17]), it turns out that, even under ultra high vacuum conditions, corresponding to oxygen partial pressures of about 10^{-12} bar, the oxygen content of the liquid phase can be largely sufficient to saturate the liquid surface.

For this reason, some studies have been made to measure the surface tension of aluminium [18] and tin [19] in an Auger spectrometer. Using this technique, by which it is possible to measure surface oxygen contents, and by ion-etching the liquid surface before each measurement, surface tension values near the melting point have been obtained, which are higher than those usually obtained even by the best experiments carried out by classical techniques.

In order to try to follow the variation in σ as a function of the oxygen content of the bulk liquid phase, we chose tin as a model metal with low oxygen solubility, sufficiently low vapour pressure from the melting point up to 1000° C, and with low reactivity with support ceramic materials (in order to use the sessile-drop technique). The availability of the recent results of the Auger experiments [19] also determined our choice.

As far as we know, no similar study on tin is available in the literature; however, quite a large number of surface tension values of tin are available [20–50], with surface tension values at the melting point (505 K) ranging from about 500 to $\sim 600\,\mathrm{mN\,m^{-1}}$ and with a comparatively high spread in the values of the temperature coefficient, $d\sigma/dT$, which ranges from 0.05 to $0.22\,\mathrm{mN\,m^{-1}\,K^{-1}}$.

This considerable scatter may be ascribed to different reasons, such as different purity levels, different degrees of accuracy of the experimental techniques, and different methods for calculating σ. But the most

0022–2461/90 $03.00 + .12

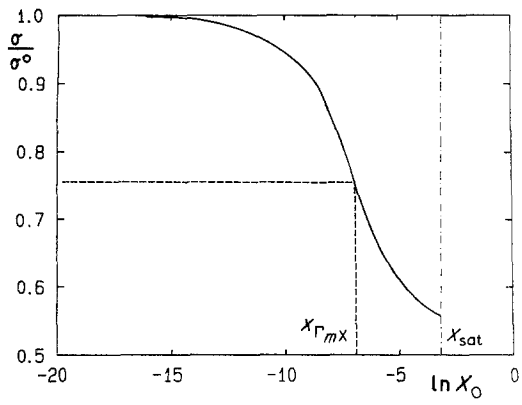

Figure 1 Typical dependence of surface tension on the logarithm of the oxygen content of the liquid phase.

important factor could be found in the composition of the measuring atmospheres, which could have had different "oxidizing" properties.

Moreover, as shown in Section 4, the fluid-dynamic conditions of the gaseous environment can affect, to a great extent, the actual oxygen exchange rate through the liquid–vapour interface.

2. Experimental procedure

The surface tensions of liquid tin and liquid tin–oxygen alloys were measured by the sessile-drop technique [51]. The drop image, obtained on a high-resolution photographic film by using the optical setup described previously [11], was processed in order to obtain the coordinates of its profile to a precision of $\pm 2\,\mu$m. The surface tension was then computed by a modified Maze and Burnet procedure [52, 53].

Experiments were performed in two furnaces. Furnace 1 consisted of a vitreous graphite inner tube, containing the test specimen, heated by high frequency (≈ 1 MHz), under vacuum conditions ($\approx 10^{-7}$ mbar) or under reduced pressure of purified helium. In this furnace, due to the presence of carbon, it was possible to obtain oxygen partial pressures lower than 10^{-25} bar in the range $300 \leqslant T(^\circ\text{C}) \leqslant 1000$. Furnace 2 was made up of a laboratory tube of vitreous silica, heated by SiC resistors up to a maximum temperature of 1150° C, either under a vacuum (10^{-6} mbar) or under different reducing or oxidizing atmospheres. In furnace 1, experiments were carried out to measure the surface tension of pure tin from its melting point to 1200° C, whereas furnace 2 was used to evaluate the dependence of σ on oxygen partial pressure.

2.1. Preparation of specimens

Marz-grade tin (analysis in Table I) was used in the form of small pieces, each weighing about 1 g. After mechanical abrasion of its surface and after cleaning with organic solvents, tin was pre-melted in furnace 1 at 800° C under vacuum on a vitreous carbon support. The drops so obtained were then used for the measurements of σ in both furnaces.

2.2. Measurement techniques

Tin sessile drops were formed on sapphire (monocrystalline Al_2O_3) substrates, 15 mm diameter, 2 mm thick, previously treated under a vacuum of 10^{-6} mbar for 2 h at 1200° C.

The specimens were introduced into the cold furnace and then heated, under a vacuum of 10^{-6} mbar, after performing a perfect alignment of the optical apparatus. The heating rate was kept below 300° C min^{-1}, due to the low thermal shock resistance of the sapphire support.

After being kept for at least 2 h at 750° C, the furnace was fluxed with the desired atmosphere (1 bar total pressure), and the drops were allowed to reach the new equilibrium conditions with a holding time of about 1 h. The temperature was then decreased by 50° C steps, and the drops were again allowed to reach the new equilibrium conditions. Photographs were taken at regular intervals.

2.3. Gaseous atmospheres

Helium, previously purified down to a maximum oxygen content of less than 1 p.p.m., was used either as a pure gas or as a mixture with hydrogen in order to obtain the desired composition of the working atmosphere. Carrier gases were always passed through a liquid nitrogen trap.

The composition of the gaseous atmosphere was monitored using a calcium-stabilized zirconia solid state gauge, placed behind the liquid drop and heated by a separate furnace. The gauge was kept at the temperature of the drop, down to 550° C, which represents the minimum working temperature of the gauge itself.

It is necessary to follow this procedure to keep account of the equilibrium reaction of water, which affects the oxygen partial pressure. Under 550° C, the gauge does not work properly, but, at the same time, the kinetics of the water reaction should also be very slow. For this reason, we regarded the P_{O_2} value at 550° C as being valid, even in the range $232 \leqslant T(^\circ\text{C}) \leqslant 550$.

3. Results

Experiments were performed under different conditions. Three types of atmosphere were used: vacuum, helium and helium + 5% hydrogen.

TABLE I Chemical analysis of tin (supplier: MRC Europe, degree of purity MARZ)

Element	p.p.m.
Ag	< 5
Al	< 5
Bi	< 5
Co	< 5
Cu	< 5
Fe	< 5
In	< 1
Mg	< 5
Ni	< 5
P	< 1
Pb	< 1.5
Si	< 5
Oxygen	< 5
Hydrogen	< 1
Nitrogen	< 5

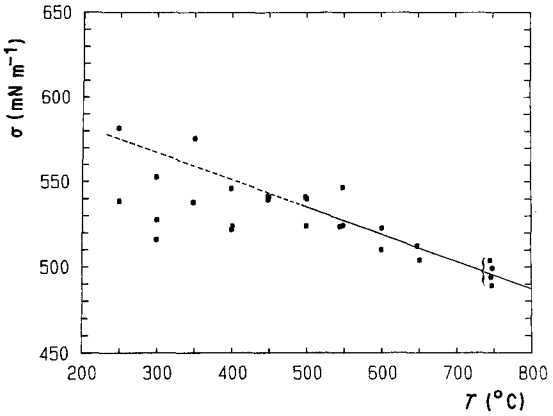

Figure 2 Experimental surface tension of tin under a vacuum.

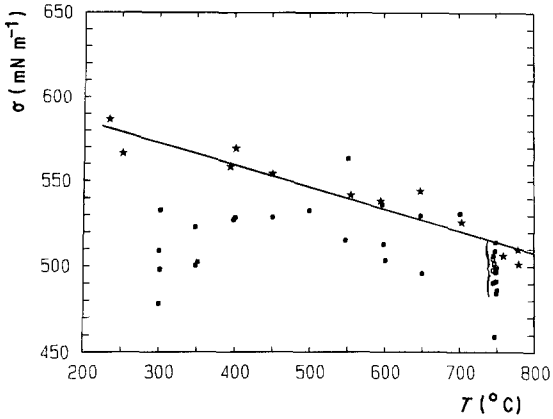

Figure 4 Experimental surface tension of tin under helium.

3.1. Vacuum

The surface tension values measured under vacuum conditions (5×10^{-6} to 1×10^{-7}) are presented in Fig. 2. The best regression line through the points at temperatures higher than 500° C gives

$$\sigma = 578 - 0.16\,(t - 232) \qquad (2)$$

with a total standard deviation SD = 8.6. The standard deviation of the slope is $SD_s = 1.3 \times 10^{-2}$. The reason why points in the low temperature range have not been included in the regression procedure is explained in Section 4. It is worth noting that in this temperature range, the points with high surface tension values also fit Equation 2.

3.2. Helium + 5% hydrogen

The points relevant to experiments performed in the presence of a gaseous flux ($0.1\,l\,min^{-1}$) of He + 5% H_2 at 1 bar total pressure are reported in Fig. 3. The best regression line through the points at $T > 450°C$ gives

$$\sigma = 562 - 7.4 \times 10^{-2}\,(t - 232) \qquad (3)$$

with a total standard deviation SD = 4.24 and a standard deviation of the slope $SD_s = 1.1 \times 10^{-2}$.

3.3 Helium

Helium atmospheres containing different oxygen percentages were fluxed over the liquid drops, at a rate of $0.1\,l\,min^{-1}$, in order to assess the influence of oxygen on the surface tension of pure tin. The results are presented in Fig. 4: they show a large scatter in the measured values, well beyond the usual degree of uncertainty of the sessile-drop method, which is always of at around 1%.

A particular behaviour can be observed in the low-temperature range. Here, surface tension very often takes on values lower than expected, if the usual linear extrapolation of the trend in the high-temperature range is applied. This behaviour has also been observed, for example, in zinc by Nogi *et al.* [54], and in Pb–Bi alloys by Maze and Burnet [55], who attributed it to evaporation effects. We shall discuss this point in detail in Section 4.

In Fig. 4, the points marked with stars are those characterized by the highest surface tension values at each temperature; they were obtained in furnace 1 and correspond to very low oxygen partial pressures. If we consider only these points, we have

$$\sigma = 581 - 0.13\,(t - 232) \qquad (4)$$

with SD = 9.1 and SDs = 1.3×10^{-2}.

Equation 4 can be regarded as evidence for the possibility of obtaining surface cleanliness when working under appropriate conditions in pure gases.

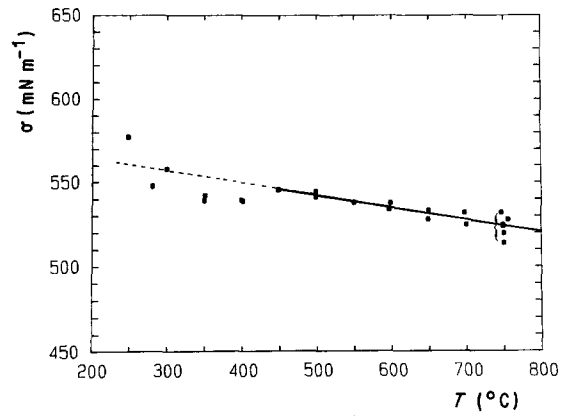

Figure 3 Experimental surface tension of tin under He + 5% H_2.

4. Discussion

The results reported above, in particular those obtained under a helium atmosphere (Fig. 4), clearly show how the surface tension of the liquid metal is affected by the presence of a tensio-active element (in our case, by oxygen). These data are then to be interpreted on the basis of the study of the thermodynamic equilibrium of the system Sn–O. However, the same results cannot be interpreted from the point of view of thermodynamic equilibrium only; it is necessary also to take into account transport properties in the gaseous phase.

4.1. Equilibrium thermodynamics

Fig. 5 shows the stability diagram of the Sn–O system for three temperatures of particular interest for our work. In general, this kind of plot illustrates the behaviour of the partial pressures of two gaseous species in equilibrium with different condensed phases. In the present case, the vertical lines correspond to the oxidation equilibrium.

$$Sn_{(l)} + O_2 = SnO_{2(c)} \qquad (5)$$

which is independent of tin vapour pressure.

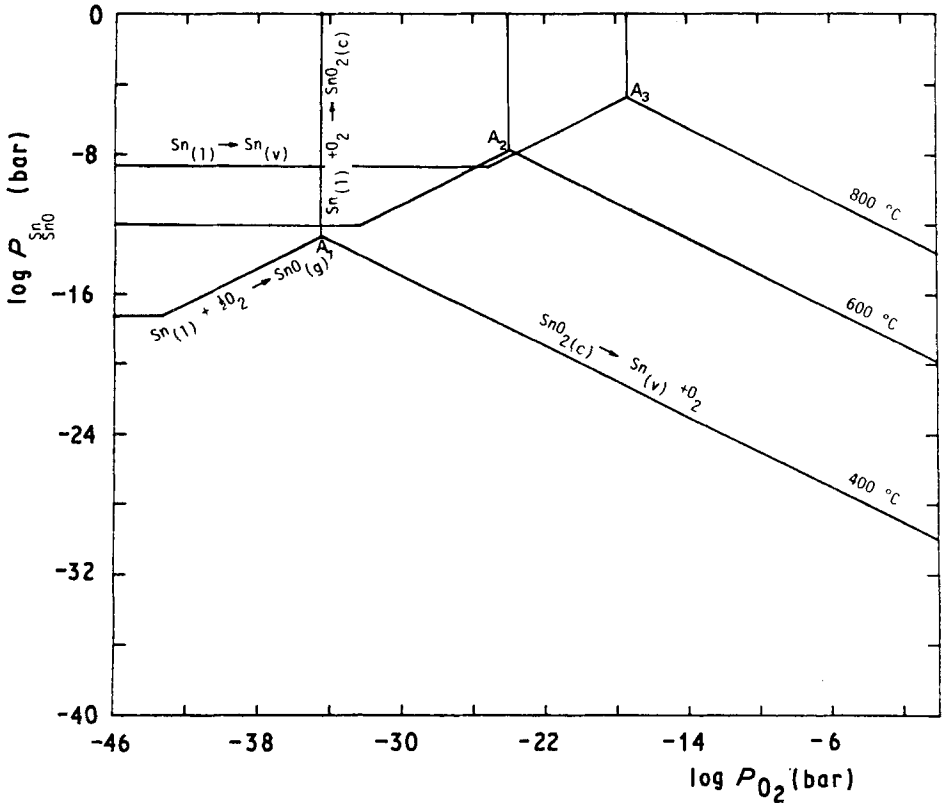

Figure 5 Volatility diagram of the Sn–O system at 400, 600 and 800° C.

Similarly, at the horizontal lines refer to the evaporation of tin equilibrium, which is independent of oxygen partial pressure. The oblique lines refer to the dissociation equilibrium

$$SnO_{2(c)} = Sn_{(g)} + O_2$$

which depends on tin vapour pressure and on oxygen partial pressure. The points A1, A2 and A3 correspond to the equilibrium oxygen pressures at the different temperatures considered. All the relevant thermodynamic values used to draw Fig. 5 have been taken from Kubaschewsky *et al.* [56], or calculated according to Coughlin [57] and the JANAF tables [58].

4.2. Kinetics of fluxes

In order to apply the equilibrium considerations already made, when dealing with metal–gas systems at high temperatures, it is necessary to consider the "real" concentration of the reactive gas that comes into contact with the liquid surface. This can be accomplished by taking into account the diffusion phenomena involved in the gas–metal interactions. These conditions have been analysed in a recent paper [59], and are summarized below.

When a liquid metal comes into contact with a fluxing gaseous phase containing a reactive component, four characteristic regimes can be defined: (a) no reactions, or slow reactions (i.e. reaction times $\gg$ diffusion times); (b) fast reactions, with an excess of oxygen atoms; (c) fast reactions, with an excess of metal vapours; (d) instantaneous reactions. Such regimes are outlined in Fig. 6.

The following reaction between oxygen and the metal M is considered.

$$\alpha(O)_{(g)} + (M)_{(l)} = (MO_\alpha)_{(s)} \qquad (6)$$

In the case of regime a, whether Reaction 6 is or is not possible, a counter diffusion of oxygen and metal vapours occurs, and the oxygen adsorption rate depends mainly on oxygen partial pressure.

In regime b, Reaction 6 is thermodynamically possible with a large availability of the reactive gas. Oxygen approaches the liquid surface and reacts with M. Only a part of oxygen dissolves in the bulk liquid, in accordance with the equilibrium partial pressure of O_2 (Reaction 6).

In regime c there is a large excess of metal vapours: nearly all O_2 molecules are "captured" far from the liquid surface, thus giving rise to a "fog" of solid oxide. However, the reaction acts as a barrier for oxygen, so that its flux reaching the liquid surface nearly vanishes.

In regime d the reaction takes places at a certain distance, Σ, from the liquid surface. Here the equilibrium partial pressure of O_2 is reached. The flux of oxygen towards the liquid metal depends on its concentration gradient which is, obviously, the smaller the greater the distance of Σ from the liquid surface.

A quantitative description of the flux regimes can be made by means of two characteristic parameters:

$$\text{Thiele modulus } \phi = \delta\{[\alpha k P_M/(P_{to} D_A)]\}^{1/2}$$

$$\dot{\varepsilon} = (\alpha P_M D_B)/(P_O D_A)$$

where P_O is the oxygen partial pressure in the fluxing gas, P_M the vapour pressure of the liquid metal, D_A the oxygen diffusivity, D_B the metal vapour diffusivity, α the stoichiometric coefficient in Reaction 6, δ the distance between the liquid–vapour interface and the unaffected gas phase.

A certain system, under specific temperature, pressure and flux rate conditions, can then be represented,

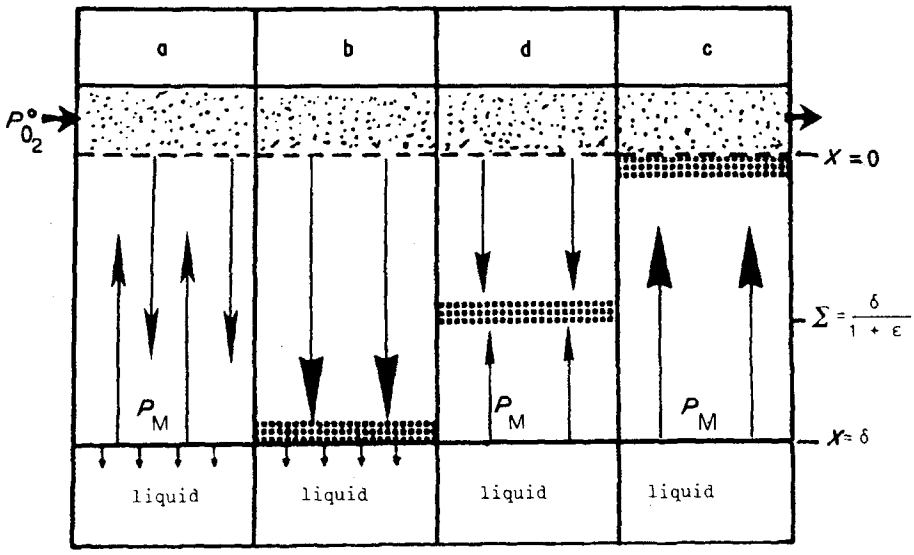

Figure 6 Schematic representation of the four reaction regimes near the liquid–vapour interface.

in the diagram lg $\dot{\varepsilon}$ against lg ϕ^2, as a point belonging to one of the specified reaction regimes.

Application of this procedure to the Sn–O system gives the results shown in Fig. 7, where the values of ϕ and $\dot{\varepsilon}$ refer to three different temperatures, for different values of the oxygen partial pressures, at a total pressure of 1 bar.

4.3. Critical assessment of the experimental results

4.3.1. Surface tension of pure tin at its melting point

As pointed out in Section 1, there is a considerable scatter in the literature values of the surface tension of tin at its melting point. The results of the present work, computed by means of the best fits under different atmospheres as mentioned previously, give $562 < \sigma\ (\mathrm{mN\,m^{-1}}) < 581$. In this range, the higher value compares very well with the results obtained by Sangiorgi *et al.* [19] for very low oxygen coverages.

4.3.2. Surface tension–temperature

4.3.2.1. Helium + 5% hydrogen. One striking difference concerning the results shown in Figs 2, 3 and 4 is that, under an atmosphere of He + 5% H_2, the experimental points show the lowest scatter from a straight line which, on the other hand, has the smallest temperature dependence. This may be explained by two considerations.

(a) In the presence of hydrogen, an oxygen partial pressure always lower than 10^{-25} bar was measured over the whole temperature range. This means that, at least down to about 500° C, tin oxide cannot be formed. Regime **a**(no reactions) conditions have then to be applied in order to calculate the interfacial fluxes; such conditions give, in accordance to the same

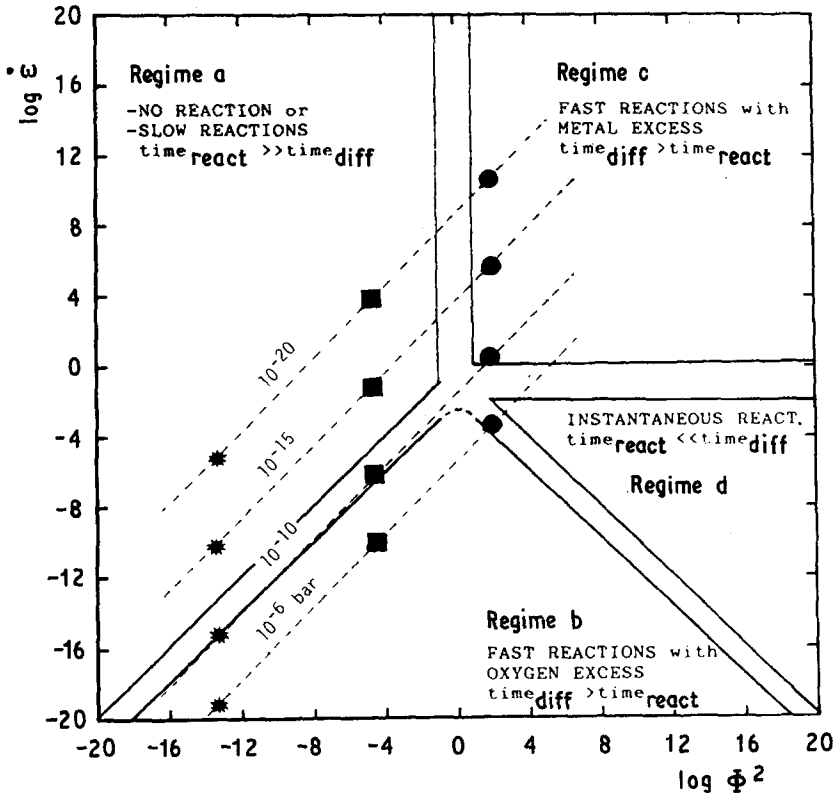

Figure 7 Diagram showing the different reaction regimes. Points refer to different oxygen partial pressures at three temperatures: (*) 232° C (melting point of tin), (■) 450° C, (●) 750° C.

treatment described by Costa *et al.* [59], exceedingly long times for monolayer formation. This means that a molten drop cannot be enriched in oxygen provided by the gaseous environment. However, at the same time, oxygen can leave the drop. This mechanism gives rise to high surface tension values (nearly clean surfaces). As temperature decreases more and more, the oxygen equilibrium pressure for oxide formation might eventually be reached, but the kinetics of this reaction strongly depends upon the net flux of oxygen atoms through the liquid–vapour interface.

(b) On the other hand, at 750° C, an equilibrium condition with some residual oxygen still dissolved into liquid tin can certainly be achieved.

Upon cooling, the saturation solubility of oxygen decreases, and its surface segregation increases, giving rise to surface tension values lower than expected. In fact, sometimes, by visual inspection of the surface of a liquid drop it was possible to notice that, at temperatures near the solidification point, the drop appeared less shining than at higher temperatures.

The above discussion can explain, at the same time, the small temperature coefficient found in this series of experiments. In fact, the fitting of the experimental points to a straight line is good at high temperatures, but it becomes worse in the low-temperature range where a convex curve could better interpolate the experimental results.

4.3.2.2. Helium atmospheres. The results reported under the heading "helium" represent a widespread population of surface tension measurements with associated values of oxygen partial pressures ranging from 10^{-5} to 10^{-20} bar (the latter value was obtained in furnace 1).

Fig 7 shows the relevant points under these conditions, at three typical temperatures; this diagram can help to interpret and clarify Fig. 4. At $P_{O_2} = 10^{-6}$ bar, all the points belong to regime b, that is "fast reactions with oxygen excess". This means that, under the flux conditions imposed on the system, oxygen can reach the liquid surface, react with it to form the oxide, and then, if time allows, saturate the liquid drop. However, at $T > 750°C$, the points enter an intermediate region towards regime d (or c), where the excess of metal vapours takes away the reaction zone from the liquid–vapour interface. Under these conditions, the amount of oxygen atoms that can reach the liquid is determined by diffusion process, which in turn depends on the concentration gradient between the "reaction surface Σ" (with the equilibrium P_{O_2} value of Reaction 6) and the liquid surface itself. For this reason, at $T > 700°C$, the liquid drops still keep a very low level of dissolved oxygen, even though thermodynamics predicts metal–oxygen reactions.

A decrease in oxygen partial pressure in the fluxing gas makes the points shift towards regimes a or c. Points with $P_{O_2} = 10^{-10}$ bar all lie in an intermediate region, where the behaviour of the system can be described as pertaining to regime a or b. At $P_{O_2} = 10^{-15}$ or 10^{-20} bar, all points but those for $T > 750°C$ belong to regime a, where no reactions are possible and where the oxygen flux is only determined by diffusion laws.

In our case, the point at $P_{O_2} = 10^{-20}$ and $T = 750°C$, also has to be assigned to this regime, in so far as the imposed oxygen pressure is lower than that corresponding to the equilibrium (Reaction 5).

In the low-temperature range the oxygen fluxes are very low (Table II) but, at temperatures above 700° C, they enter a measurable range.

Isothermal runs were performed at $T = 750°C$, lasting up to 50 h. The results, enclosed within brackets, are shown in Figs 2, 3 and 4: a regular increase in surface tension from low values to higher values has been obtained, but a definite trend towards a unique high value has never been observed. Rather, an oscillation has been noticed around a value which is very near the best-fit interpolated line.

This behaviour is consistent with the "statistical" aspect of the kinetic equilibrium due to diffusion processes.

5. Conclusions

1. Oxygen affects the surface tension of molten tin. Its effect is stronger in the temperature range near the melting point, where the surface tension varies from $\sigma \approx 470\,mN\,m^{-1}$ for an oxidized surface, to $\sigma \approx 580\,mN\,m^{-1}$ for a surface in equilibrium with very low oxygen pressures ($P_{O_2} < 10^{-20}$ bar).

2. To evaluate the effect of a gaseous environment on the surface tension of tin, it is not sufficient to consider equilibrium conditions alone; the conditions related to the kinetics of gaseous (vapour) fluxes must also be taken into account. This approach can be basic to the design of appropriate set-ups for measuring surface tensions of liquid metals.

3. If the conditions for preventing oxygen from reaching the liquid tin surface are fulfilled, the

TABLE II Oxygen fluxes at the liquid–vapour interface

P_{O_2} (bar)	$T_1 = 450°C$			$T_2 = 750°C$		
	N (mol cm^{-2} sec^{-1})	t_m^* (sec)	Regime	N (mol cm^{-2} sec^{-1})	t_m^* (sec)	Regime
10^{-6}	1.7×10^{-12}	0.50	b	1.2×10^{-12}	0.72	b or d
10^{-10}	1.7×10^{-16}	5.1×10^{3}	b or d	9.3×10^{-13}	0.89	c
10^{-15}	1.7×10^{-21}	5.1×10^{8}	a	3.13×10^{-17}	2.7×10^{4}	c
10^{-20}	1.7×10^{-26}	5.1×10^{13}	a	1.16×10^{-26}	7.2×10^{13}	c
10^{-25}	1.7×10^{-31}	5.1×10^{18}	a	1.16×10^{-31}	7.2×10^{18}	c

*Time required to obtain an oxygen monolayer of unit area (1 cm^2).

following law describing the variation of surface tension with temperature holds true

$$\sigma = 581 - 0.13\,(t - 232)$$

with a degree of accuracy of $\pm 1\%$. This equation can be regarded as an accurate evaluation of the surface tension of pure tin as a function of temperature.

References

1. B. J. KEENE, *Int. Mater. Rev.* **33** (1988) 1.
2. K. OGINO and H. TAIMATSU, *J. Jpn. Inst. Metals* **43** (1979) 871.
3. K. OGINO, H. TAIMATSU and F. NAKATANI, *ibid.* **46** (1982) 957.
4. G. BERNARD and C. H. LUPIS, *Metall. Trans.* **2** (1971) 2991.
5. R. SANGIORGI, M. L. MUOLO and A. PASSERONE, *Acta Metall.* **30** (1983) 1597.
6. H. TAIMATSU, M. ABE, F. NAKATANI and K. OGINO, *J. Jpn. Inst. Metals* **49** (1985) 523.
7. K. MONMA and H. SUTO, *Trans. Jpn. Inst. Metals* **2** (1961) 149.
8. T. E. O'BRIEN and C. D. CHAKLADER, *J. Amer. Ceram. Soc.* **57** (1974) 329.
9. Z. MORITA and A. KASAMA, *J. Jpn. Inst. Metals* **40** (1976) 787.
10. B. GALLOIS and C H. LUPIS, *Metall Trans. B* **12** (1981) 549.
11. A. PASSERONE, R. SANGIORGI and G. CARACCIOLO, *J. Chem. Thermodyn.* **15** (1983) 971.
12. D. H. BRADHURST and A. S. BUCHANAN, *J. Phys. Chem.* **63** (1959) 1486.
13. J. C. HARDY, *J. Crystal Growth* **69** (1984) 456.
14. *Idem ibid,* **71** (1985) 602.
15. C. GARCIA-CORDOVILLA, E. LOUIS and A. PAMIES, *J. Mater. Sci.* **21** (1986) 2787.
16. E. RICCI, A. PASSERONE and J. C. JOUD, *Surf. Sci.* **206** (1988) 533.
17. O. OTZUKA and Z. KOZUKA, *Trans. Jpn. Inst. Metals* **22** (1981) 558.
18. L. GOUMIRI and J. C. JOUD, *Acta metall.* **30** (1982) 1397.
19. R. SANGIORGI, C. SENILLOU and J. C. JOUD, *Surf. Sci.* **202** (1988) 509.
20. M. J. MURTHA and G. BURNET, in "An Annotated Bibliography for Liquid Metal Surface Tension of Groups 3A, 4A and 5A Metals", IS 3829 Report, Ames Library, ERDA (Iowa State University, Ames 50011 Iowa, April 1976).
21. G. LANG, *J. Inst. Metals* **101** (1973) 300.
22. F. H. HOWIE and E. D. HONDROS, *J. Mater. Sci.* **17** (1982) 143.
23. D. W. G. WHITE, *Metall. Trans.* **2** (1971) 3067.
24. H. K. ABOL ABDEL-AZIZ, M. B. KIRSHAH and A. M. AREF, *Z. Metallkde.* **66** (1975) 183.
25. J. A. CAHILL and A. D. KIRSHENBAUM, *J. Inorg. Nucl. Chem.* **26** (1964) 206.
26. I. LAUERMANN, G. METZGER and F. SAUERWALD, *Z. Phys. Chem. (Leipzig)* **216** (1961) 42.
27. K. MUKAI, I. KASHIWAGI and T. TAKANORI, *Jpn Bull. Kyushu Technol.* **26** (1973) 155.
28. YU. V. NAIDICH, V. M. PEREVERTAILO and V. S. ZHURAVLEV, *Russ. J. Phys. Chem.* **45** (1975) 556.
29. N. L. POKROVSKII and N. D. GALANINA, *Zh. Fiz. Khim.* **23** (1949) 324.
30. N. L. POKROVSKII and D. S. TISSEN, *Proc. Akad. Nauk SSSR Phys. Chem.* **128** (1959) 879.
31. *Idem, Russ. J. Phys. Chem.* **34** (1960) 592.
32. N. L. POKROVSKII and M. SAIDOV, *Z. Fiz. Khim.* **29** (1955) 1601.
33. N. L. POKROVSKII, P. P. PUGACHEVICH and KH. I. IBRAGIMOV, *Sov. Phys. Dokl.* **12** (1967) 170.
34. A. E. SCHWANEKE, W. L. FALKE and V. L. MILLER, *J. Chem. Engng. Data.* **23** (1978) 298.
35. L. L. BIRCUMSHAW, *Phil. Mag.* **17** (1934) 181.
36. D. A. MELFORD and T. P. HOAR, *J. Inst. Metals* **85** (1957) 197.
37. Y. MATUYAMA, *Sci. Rep. Tohoku Imp. Univ.* **16** (1927) 555.
38. G. DRATH and F. SAUERWALD, *Z. Anorg. Chem.* **162** (1927) 301.
39. G. LANG, P. LATY, J. C. JOUD and P. DESRE, *Z. Metallkde* **67** (1977) 113.
40. S. I. POPEL, I. N. KOZHORKOV and T. V. ZAKAROVA, *Zashita Metallov.* **7** (1971) 421.
41. T. P. HOAR and D. A. MELFORD, *Trans. Faraday Soc.* **53** (1957) 316.
42. T. HOGNESS, *J. Amer. Soc.* **43** (1921) 1621.
43. A. ADACHI, Z. MORITA, P. KITA, A. KASAMA and S. HUMAMATSU, *Tech. Rept. Osaka Univ.* **22** (1972) 93.
44. F. L. HARDING and D. R. ROSSINGTON, *J. Amer. Ceram. Soc.* **53** (1970) 87.
45. E. PELZEL, *Berg. Huettemaenn Monatsh.* **93** (1948) 248.
46. B. C. ALLEN and W. D. KINGERY, *Trans. Met. Soc. AIME* **215** (1969) 30.
47. S. M. KAUFMANN and T. J. WHALEN, *Acta Metall.* **13** (1965) 797.
48. M. DEMERI, M. FARAG and J. HEASLEY, *J. Mater. Sci.* **9** (1974) 683.
49. D. V. ATTERTON and T. P. HOAR, *J. Inst. Metals* **81** (1953) 541.
50. D. R. SAGEMAN, PhD Thesis, Library Iowa State University, Ames, Iowa, 1976, unpublished.
51. J. F. PADDAY, in "Surface and Colloid Science", edited by E. Matijevic Vol. 1 (Wiley-Interscience, New York, 1969) p. 101.
52. C. MAZE and G. BURNET, *Surf. Sci.* **13** (1969) 451.
53. *Idem, ibid.* **24** (1971) 335.
54. K. NOGI, K. OGINO, A. MCLEAN and W. A. MILLER, *Metall. Trans.* **17B** (1986) 163.
55. C. MAZE and G. BURNET, *Surf. Sci.* **27** (1971) 411.
56. O. KUBASCHEWSKY and C. B. ALCOCK, "Metallurgical Thermochemistry", 5th Edn (Pergamon, Oxford, New York, 1979).
57. J. P. COUGHLIN, *Bur. Mines Bull.* **542** (1954) 1.
58. JANAF Thermochemical Tables (National Bureau of Standards, 1971) and supplement (1974).
59. P. COSTA, A. PASSERONE and E. RICCI, *High Temp. High Press.* **20** (1988) 59.

Received 17 May
and accepted 26 September 1989